Plant Physiol. (1997) 114: 605–613

ATP Hydrolysis Activity and Polymerization State of Ribulose-1,5-Bisphosphate Carboxylase Oxygenase Activase[1]

Do the Effects of Mg^{2+}, K^+, and Activase Concentrations Indicate a Functional Similarity to Actin?

Ross McC. Lilley* and Archie R. Portis, Jr.

Department of Biological Sciences, University of Wollongong, Northfields Avenue, Wollongong 2522, Australia (R.M.L.); and Photosynthesis Research Unit, Agricultural Research Service, United States Department of Agriculture and Department of Crop Sciences, University of Illinois, Urbana, Illinois 61801–3838 (A.R.P.)

The ATPase activity and fluorescence of ribulose-1,5-bisphosphate carboxylase oxygenase (Rubisco) activase were determined over a range of $MgCl_2$, KCl, and activase concentrations. Both salts promoted ADP release from ATP and intrinsic fluorescence enhancement by adenosine 5′-[γ-thio] triphosphate, but Mg^{2+} was about 10 times more effective than K^+. ATPase and fluorescence enhancement both increased from zero to saturation within the same Mg^{2+} and K^+ concentration ranges. At saturating concentrations (5 mM Mg^{2+} and 22 mM K^+), the specific activity of ATPase (turnover time, about 1 s) and specific intrinsic fluorescence enhancement were maximal and unaffected by activase concentration above 1 μM activase; below 1 μM activase, both decreased sharply. These responses are remarkably similar to the behavior of actin. Intrinsic fluorescence enhancement of Rubisco activase reflects the extent of polymerization, showing that the smaller oligomer or monomer present in low-salt and activase concentrations is inactive in ATP hydrolysis. However, quenching of 1-anilinonapthaline-8-sulfonate fluorescence revealed that ADP and adenosine 5′-[γ-thio] triphosphate bind equally well to activase at low- and high-salt concentrations. This is consistent with an actin-like mechanism requiring a dynamic equilibrium between monomer and oligomers for ATP hydrolysis. The specific activation rate of substrate-bound decarbamylated Rubisco decreased at activase concentrations below 1 μM. This suggests that a large oligomeric form of activase, rather than a monomer, interacts with Rubisco when performing the release of bound ribulose-1,5-bisphosphate from the inactive enzyme.

Rubisco activase is a soluble protein of 41 to 45 kD that occurs in the chloroplast stroma of algae and higher plants (Salvucci et al., 1987) and, on the basis of gene sequences, in cyanobacteria (Li and Tabita, 1994). The tertiary structure of the activase monomer protein and the quaternary structure of its polymer have not been determined. Rubisco activase enhances the rate and extent of activation of the carbon-fixing enzyme Rubisco by facilitating the release of sugar phosphates from decarbamylated and catalytically inactive Rubisco (for reviews, see Portis [1990, 1992]; Salvucci and Ogren [1996]). Decarbamylated Rubisco binds its substrate, RuBP, very tightly (Jordan and Chollet, 1983; Portis, 1992) and without activase, the inactive complex formed in the chloroplast stroma under some conditions, such as following a sudden transition from high to low light (Brooks and Portis, 1988), would persist for long periods. Additionally, during normal catalysis Rubisco accumulates tight-binding inhibitors arising from the occasional formation of other pentose bisphosphates by epimerization of the ene-diol form of RuBP on the active site (Edmondson et al., 1990; Andrews et al., 1995). The mechanism by which Rubisco activase binds with the Rubisco-pentose bisphosphate complex and releases RuBP or inhibitor is not known. In higher plants there are two closely related forms of Rubisco activase, which have molecular masses of 42 and 45 kD in spinach and exhibit different kinetics toward ATP concentration (Shen et al., 1991), whereas in *Chlamydomonas reinhardtii* activase is present as a single polypeptide (Roesler and Ogren, 1990).

Rubisco activase exhibits an ATPase activity that is apparently not directly connected to the activation of RuBP-bound Rubisco. This activity is highly specific for Mg-ATP, exhibits a sigmoidal response to ATP concentration, and is inhibited by ADP (Robinson and Portis, 1989). Rubisco activase forms oligomers of a size dependent on the concentration of Mg^{2+} and the adenine nucleotide present. Wang et al. (1993) used gel filtration to obtain size estimates of Rubisco activase and found an apparent molecular mass of 340 kD with 100 μM ADP plus 5 mM Mg^{2+}, corresponding to an oligomer of about 8 subunits. With 200 μM ATP plus 5 mM Mg^{2+}, the apparent size of the oligomer increased to more than 14 subunits, but substantial size polydispersity, indicated by skewed column peaks, was always present. With slower separation procedures occupying many hours and using columns or gradient centrifugation in the absence of added adenine nucleotides, Rubisco activase dissociates into a near-monomeric state,

[1] This work was supported in part by U.S. Department of Energy grant no. DE-AI02-94ER20154.

* Corresponding author; e-mail rossl@uow.edu.au; fax 61–42–21–4135.

Abbreviations: ANS, 1-anilinonapthaline-8-sulfonate; ATP-γ-S, adenosine 5′-[γ-thio] triphosphate; RuBP, ribulose-1,5-bisphosphate.

as indicated by an apparent average molecular mass of 58 kD (Salvucci, 1992).

When irradiated at 296 nm, Rubisco activase exhibits intrinsic fluorescence, which, in the presence of Mg^{2+}, is enhanced by ATP but quenched by the further addition of ADP (Wang et al., 1993). This enhancement is stabilized by the addition of an ATP-regenerating system or of the ATP analog ATP-γ-S, which is apparently bound to, but not hydrolyzed by, Rubisco activase. The degree of enhancement reflects a structural change in the protein, affecting the hydrophobicity of the environment of one or more of its four tryptophane residues, and related to the extent of aggregation of the activase monomers (Wang et al., 1993).

These findings demonstrate that the ATPase activity and the extent of oligomerization of Rubisco activase are closely linked. They also highlight a problem arising from the fact that the activase oligomerization state is influenced by the ionic environment and by activase concentration. Any attempt to determine the polymerization state by procedures such as gel-column chromatography, native-gel electrophoresis, or gradient centrifugation must alter these conditions and perturb the existing degree of polymerization. Intrinsic fluorescence is the one noninvasive procedure available for monitoring the extent of oligomerization and thus was selected for the current study. A second application of fluorescence to the study of Rubisco activase is based on ANS, a useful reporter group for monitoring ligand binding to proteins. Wang and Portis (1991) utilized ANS to study adenine nucleotide binding to activase. ANS fluorescence is modulated by nucleotide binding and by protein conformational changes associated with that binding.

The ATPase and Rubisco activation activities of Rubisco activase are strongly influenced by Mg^{2+}. This protein contains two tightly bound Mg^{2+} ions per activase monomer, which are not removed by precipitation with ammonium sulfate in the presence of EDTA (Frasch et al., 1995). The concentration of Mg^{2+} in the chloroplast stroma is light-dependent and is of regulatory significance for other reactions of the Benson-Calvin cycle (Gardemann et al., 1986). Additionally, K^+ is included in assays of the ATPase activity of Rubisco activase (see Robinson et al., 1988). However, the effect on Rubisco activase activity of K^+, a major cation of the internal cellular environment, has not been investigated.

The aim of this work is to examine the effects of these two cations and of activase concentration on the ATPase (we use the term "ADP release," since ADP- or Pi-bound protein are often intermediates of ATP hydrolysis) and on the extent of polymerization as determined by intrinsic fluorescence enhancement by ATP-γ-S. Since the function and stoichiometry of the two forms of Rubisco activase are unknown, we have based our study on the 42-kD form, which was expressed and purified from the cloned gene. We define conditions in which intrinsic fluorescence enhancement by ATP-γ-S is close to zero and others in which it is maximal. We compare the binding of adenine nucleotides with Rubisco activase under some of these defined conditions, and we determine the rate of activation of Rubisco over a range of activase concentrations associated with a changing polymerization state.

MATERIALS AND METHODS

Preparation of Rubisco Activase

Rubisco activase from spinach (*Spinacea oleracea*) was overexpressed in *Escherichia coli* harboring pPlex 1.6 and purified essentially by the procedures of Shen et al. (1991), except that the culture was grown at 37°C. After cell lysis, activase was precipitated in 35% ammonium sulfate, desalted by gel filtration, and then subjected to anion-exchange chromatography. Rubisco activase was located in column fractions that exhibited ATPase activity but not glycerate 3-P hydrolysis, and was confirmed by SDS-PAGE to be a 42-kD protein. Pooled activase fractions were subjected to concentrating dialysis in a pressure cell (Amicon, Beverly, MA) using a YM-30 membrane. Five cycles of concentration by a factor of 5 and dilution with 20 mM bis-Tris propane-Cl^-, 0.2 mM ATP (pH 8.0) reduced the NaCl concentration in the sample to less than 1 mM. Aliquots of the final concentrated sample were snap-frozen in liquid nitrogen and stored at −80°C.

Rate of ATP Hydrolysis

The rate of ADP release was followed using a spectrophotometric assay coupled to NADH oxidation via pyruvate kinase and lactate dehydrogenase. Reactions were initiated by the addition of Rubisco activase into a reaction mixture containing (final concentrations) 2 mM K^+ EPPS (*N*-[2 hydroxyethyl] piperazine-*N'*-[3-propane sulfonic acid]), 10 μM EDTA, 170 μM ATP, 840 μM phospho*enol* pyruvate, 300 μM NADH, 23.4 units of lactate dehydrogenase, and 15.2 units of pyruvate kinase (pH 8.0) in a final volume of 700 μL at 25°C, plus $MgCl_2$, KCl, and activase concentrations as specified. The reaction was started by adding activase, and the extinction over the wavelength range of 330 to 350 nm was determined with a diode-array spectrophotometer (Hewlett-Packard; integration time, 0.2 s; cycle time, 1 s). The extinction coefficient for NADH over this wavelength range was determined to be 6.01 mM^{-1}. The concentrations of ATP and Mg^{2+} that are given refer to total concentrations with no correction for binding.

In every experiment the performance of the coupling system was verified by the addition of an aliquot containing 21 nmol of ADP at the end of the observed time course. Following this addition, the initial rate of NADH oxidation was at least two orders of magnitude higher than the preceding activase-dependent rates, confirming the coupling system activity. The observed equivalence of the amounts of NADH consumed and ADP in the aliquot verified the completeness of coupling.

Intrinsic Fluorescence Enhancement

The intrinsic fluorescence of Rubisco activase was determined using a spectrofluorimeter (model LS-5, Perkin-Elmer) with excitation and emission wavelengths of 296

and 345 nm, respectively (Wang et al., 1993). Reaction mixtures contained 2 mM K^+ EPPS, 10 μM EDTA (pH 8.0) in a final volume of 2.5 mL at 25°C, plus $MgCl_2$, KCl, and activase concentrations as specified. The fluorescence intensity was first measured in the absence of ATP-γ-S, then, after the addition (100 μM) of this adenine nucleotide analog, the increase in fluorescence intensity (enhancement) was determined. The specific fluorescence enhancement was calculated as instrument units per micromolar activase.

ANS Fluorescence Quenching as a Measure of Nucleotide Binding by Activase

The ability of Rubisco activase to bind the adenine nucleotides ADP and AMP and the ATP analog ATP-γ-S was determined using the fluorescent probe ANS with the spectrofluorimeter, and excitation and emission wavelengths of 380 and 480 nm, respectively (Wang and Portis, 1991). Reaction mixtures contained 2 mM K^+ EPPS, 10 μM EDTA, 1.34 μM Rubisco activase (pH 8.0) in a final volume of 2.5 mL at 25°C, plus $MgCl_2$, KCl, and activase concentrations as specified. Each reaction mixture was titrated in the presence and absence of adenine nucleotide or analog by the stepwise addition of ANS, and the fluorescence was determined over the range of 0 to 40 μM ANS.

Determination of Rubisco Activation

Rubisco activity was followed by continuous measurement of glycerate 3-P formation using the spectrophotometric assay coupled to NADH oxidation via glycerate 3-phosphate kinase and glyceraldehyde 3-phosphate dehydrogenase. Spinach Rubisco, prepared by the method of Wang et al. (1992), was converted to the decarbamylated and RuBP-bound form by gel filtration (Sephadex G50) in 50 mM Na^+ Tricine, 0.1 mM EDTA, pH 8.0. RuBP was added to the eluted Rubisco fraction to 0.2 mM. The reaction mixture contained 50 mM K^+ Tricine, 0.2 mM EDTA, 10 mM $NaHCO_3$, 10 mM $MgCl_2$, 2 mM DTT, 2.5 mM phosphocreatine, 4 mM RuBP, 2.5 mM ATP, 300 μM NADH, 100 μg mL^{-1} Rubisco (1.43 μM active sites), 10 units mL^{-1} glycerate 3-phosphate kinase, 5 units mL^{-1} glyceraldehyde 3-phosphate dehydrogenase, 10 units mL^{-1} creatine phosphokinase, and activase as specified, pH 8.1, in a final volume of 700 μL. In some reactions the concentrations of glycerate 3-phosphate kinase, glyceraldehyde 3-phosphate dehydrogenase, and creatine phosphokinase were doubled. The reaction was started by the penultimate addition of activase with stirring, a 30-s preincubation, and the addition of Rubisco with stirring. The oxidation of NADH was followed spectrophotometrically, as described for ATP hydrolysis. The performance of the coupling system was verified by the addition of aliquots containing 10 nmol of glycerate 3-P.

RESULTS

The rate of ADP release from ATP was strongly affected by the concentration of Mg^{2+} and K^+ in the assay mixture (Fig. 1). After the addition of 2.44 μM activase to a reaction mixture containing final concentrations of 5 mM Mg^{2+} and 22 mM K^+ (high-salt, trace 1), ADP release commenced

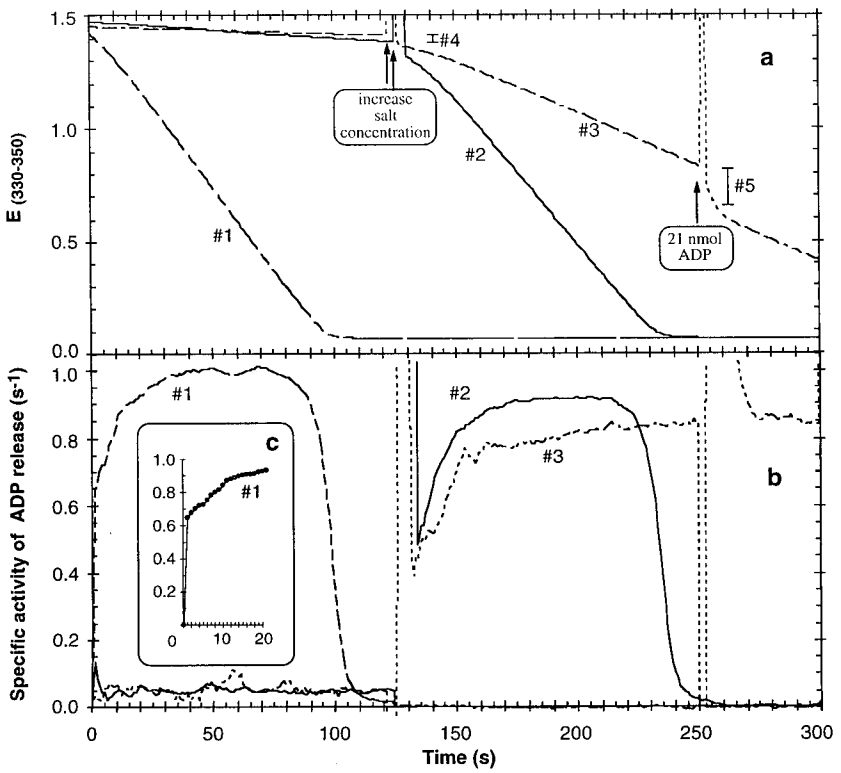

Figure 1. a, Spectrophotometric time courses of extinction (330–350 nm) during NADH oxidation coupled to ADP formation (see "Materials and Methods"). The traces, shown as continuous lines, represent raw data sampled at 1-s intervals. The brief excursions of the traces resulted from momentary stirrer insertion accompanying the addition of solutions to the cuvette. Trace 1, High-salt (5 mM $MgCl_2$, 22 mM KCl), 2.4 μM activase. Trace 2, Low-salt (0.1 mM $MgCl_2$, 5 mM KCl), 2.44 μM activase. At 125 s, the ionic concentrations were increased to high-salt by the addition of 20.2 μL of solution containing 176 mM $MgCl_2$, 612 mM KCl. Trace 3, Low-salt, 0.978 μM activase. At 122 s, the concentrations were increased to high-salt as before. At 251 s, 5 μL of a solution containing 21 nmol ADP was added. Vertical bar 4 represents the expected decrease in extinction due to dilution from salt addition. Vertical bar 5 represents the expected decrease in extinction due to the consumption of 21 nmol NADH. b, Time courses of specific activity of ADP release (mol ADP formed.mol^{-1} activase.s^{-1} or s^{-1}) calculated from the data of a. c, Expanded time course of specific activity of ADP release (s^{-1}) for trace 1.

within the 1st s (Fig. 1c). The rate of ADP release increased further over 40 s. The average plateau rate achieved (e.g. between 40 and 70 s) under these conditions was normally taken as the control (100%) specific activity (Fig. 1b) and was in the vicinity of 1 mol ADP formed.mol^{-1} activase.s^{-1}. After 80 s the rate fell off as NADH approached depletion (Fig. 1a, trace 1).

Under low-salt conditions (0.1 mM Mg^{2+} and 5 mM K^+), the specific activity of ADP release was less than 5% of that at high-salt concentrations (Fig. 1b, traces 2 and 3). The determination of the rate of ADP-dependent NADH oxidation by the addition of 21 nmol of ADP (data not shown) showed that the activity of the coupling system was attenuated in these low-salt conditions, probably primarily due to the K^+ requirement of pyruvate kinase (Boyer, 1962). Nevertheless, the coupling system activity still exceeded, by more than 1 order of magnitude, the maximum rate of activase-dependent NADH oxidation observed under these low-salt conditions. Salt concentrations lower than 0.1 mM Mg^{2+} and 5 mM K^+ were not used because at these concentrations attenuation of the coupling system would begin to affect the ADP/NADH stoichiometry.

When the conditions were changed from low- to high-salt after 120 s (by increasing the concentrations of Mg^{2+} from 0.1 to 5 mM and of K^+ from 5 to 22 mM; Fig. 1, trace 2), the rate of ADP release increased gradually and reached an approximately steady rate after about 50 s (Fig. 1b). This rate was 80 to 90% of the rate achieved when these higher concentrations of Mg^{2+} and K^+ were present from the start. There was no sign of a step increase in the amount of NADH oxidized upon salt addition, which would be expected if the reaction mixture contained unconsumed ADP. This confirms that the low activase-dependent activity observed in the low-salt conditions was not an artifact of coupling system inactivation. When the experiment of trace 2 was repeated with a lower activase concentration of 0.98 μM (trace 3), a similar result with a slightly lower rate of ADP release was observed. The addition of 21 nmol of ADP (trace 3) verified the activity of the coupling system.

The rate of ADP release by activase was determined for a range of Mg^{2+} and K^+ concentrations. When Mg^{2+} was increased in the presence of 5 mM K^+, the specific activity of ADP release increased linearly up to 2 mM Mg^{2+}, remaining approximately constant, with further increases to

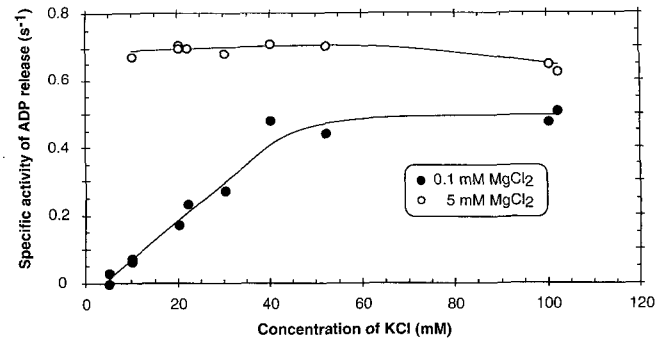

Figure 3. Effect of KCl concentration on the specific activity of ADP release from ATP (s^{-1}). ●, 0.1 mM $MgCl_2$, 0.49 μM activase; ○, 5 mM $MgCl_2$, 0.48 μM activase.

10 mM Mg^{2+}. At Mg^{2+} concentrations between 5 and 10 mM, there was no effect on the specific activity of ADP release when K^+ was increased to 22 mM (Fig. 2). The highest ATPase rates observed represent a turnover time of about 1 s.

When K^+ was increased from 5 to 40 mM in the presence of 0.1 mM Mg^{2+}, the specific activity of ADP release increased linearly to about 0.5 s^{-1} at 40 mM K^+, but was not further enhanced at 102 mM K^+ (Fig. 3). However, at all K^+ concentrations between 10 and 102 mM, the addition of $MgCl_2$ to bring the Mg^{2+} concentration to 5 mM increased the specific activity of ADP release to about 0.7 s^{-1} (Fig. 3).

When the rate of ADP release was determined for a range of activase concentrations at 5 mM Mg^{2+} and 22 mM K^+, the specific activity decreased substantially at activase concentrations below 1 μM (Fig. 4). At higher activase concentrations, the specific activity approached a constant value. With 0.1 mM Mg^{2+} and 5 mM K^+, the specific activity of ADP release showed a slight response to the activase concentration, but reached a maximum of only 7% of the activity at the higher salt concentrations. (Fig. 4).

The enhancement of intrinsic fluorescence by ATP-γ-S (instrument units per micromolar of activase) was taken as a measure of the specific intrinsic fluorescence. In the absence of added Mg^{2+}, no enhancement of fluorescence was observed despite the addition of up to 100 mM K^+ (Figs. 5 and 6). As Mg^{2+} was increased, the specific fluorescence enhancement intensity increased largely within the Mg^{2+}

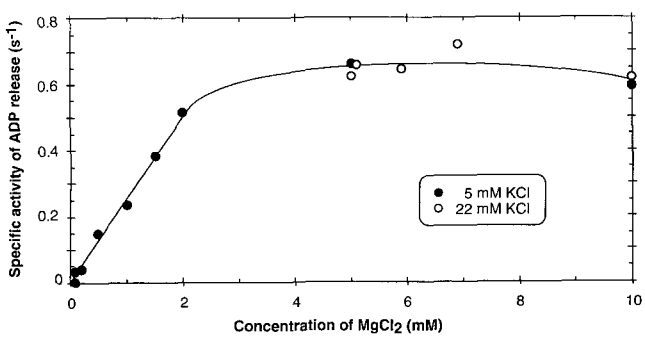

Figure 2. Effect of $MgCl_2$ concentration on the specific activity of ADP release from ATP (s^{-1}). ●, 5 mM KCl, 0.49 μM activase; ○, 22 mM KCl, 0.48 μM activase.

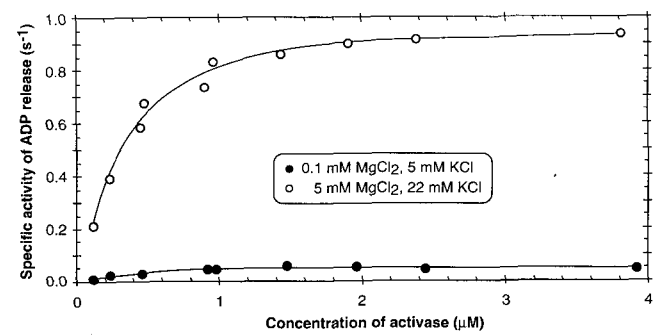

Figure 4. Effect of activase concentration on the specific activity of ADP release from ATP (s^{-1}). ●, 0.1 mM $MgCl_2$ and 5 mM KCl; ○, 5 mM $MgCl_2$ and 22 mM KCl.

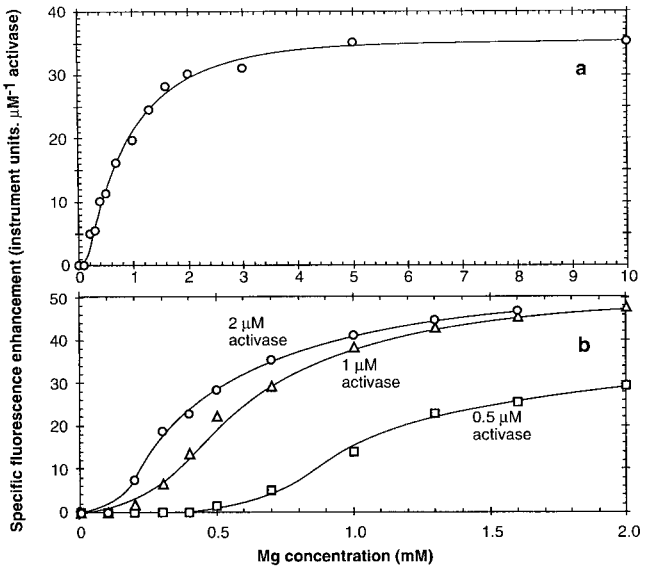

Figure 5. Effect of $MgCl_2$ concentration on the enhancement of specific intrinsic fluorescence of activase by ATP-γ-S (see "Materials and Methods"). a, 5 mM KCl, 0.44 μM activase; b, 2 mM KCl; □, 0.5 μM activase; Δ, 1 μM activase; and ○, 2 μM activase.

concentration range of 0.1 to 2 mM (Fig. 5a). The response of specific fluorescence enhancement to Mg^{2+} concentration was dependent on Rubisco activase concentration, but generally exhibited a sigmoid relationship (Fig. 5b). In the presence of 0.1 mM Mg^{2+} and 0.5 μM activase, specific fluorescence enhancement increased in a sigmoid manner with K^+ over the 5 to 40 mM K^+ concentration range, with a maximum at about 60 mM K^+ (Fig. 6). In the presence of 5 mM Mg^{2+}, 20 mM K^+, and 1 μM activase, 100 μM ADP did not enhance fluorescence and was inhibitory to the enhancement by ATP-γ-S (data not shown).

The specific fluorescence enhancement was constant above 1 μM activase concentration, but fell rapidly as the concentration decreased below this value (Fig. 7). At 25 nM activase the specific fluorescence enhancement was 13% of that at activase concentrations above 1 μM.

The ability of Rubisco activase to bind the adenine nucleotides ADP and AMP and the ATP analog ATP-γ-S was investigated using the fluorescent probe ANS under two

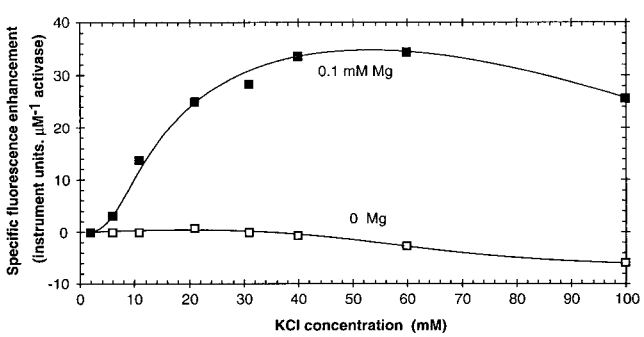

Figure 6. Effect of KCl concentration on the enhancement of specific intrinsic fluorescence by ATP-γ-S with 0.5 μM activase. □, No added $MgCl_2$; and ■, 0.1 mM $MgCl_2$.

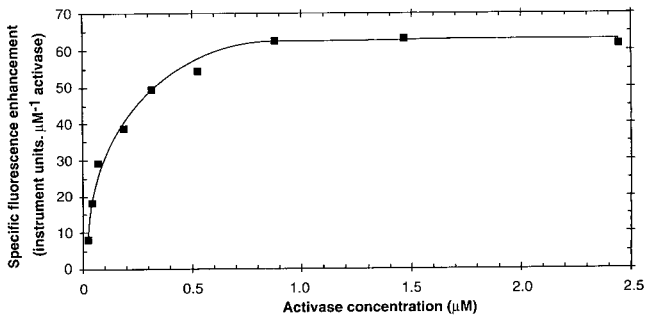

Figure 7. Effect of activase concentration on the enhancement of specific intrinsic fluorescence by ATP-γ-S with 5 mM $MgCl_2$ and 20 mM KCl.

conditions, 0.1 mM Mg^{2+} and 5 mM K^+ (low-salt) and 5 mM Mg^{2+} and 22 mM K^+ (high-salt). As the concentration of ANS was increased, the fluorescence with Rubisco activase increased almost linearly; the fluorescence intensity was higher in the high-salt conditions (Fig. 8, a–c). When 200 μM ADP was present the fluorescence decreased in both low- and high-salt conditions (Fig. 8b); the proportion of the fluorescence that was quenched was similar for both conditions (Fig. 8e). AMP at the same concentration had no significant effect on activase-ANS fluorescence (Fig. 8, c and f). ATP-γ-S (100 μM) quenched ANS fluorescence by about 50% under high-salt conditions in a manner similar to 200 μM ADP (Fig. 8, a and d). Under low-salt conditions, however, the quench profile was different (Fig. 8d) and the maximum extent of quenching of about 20% was reached at 8 μM ANS. Further increases in ANS concentration to 56 μM did not increase the degree of quenching but, rather, slightly decreased it (data not shown).

The effect of activase concentration on the rate of activation of Rubisco carboxylase was determined by the spectrophotometric method in an assay mixture containing 10

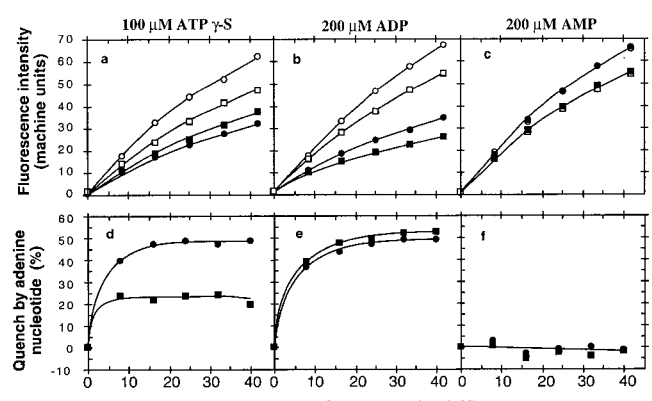

Figure 8. Quenching of ANS fluorescence with 1.34 μM activase by adenine nucleotides (see "Materials and Methods"). a–c, Fluorescence intensity with increasing ANS concentration; d–f, percent quench by adenine nucleotide; a and d, 100 μM ATP-γ-S; b and e, 200 μM ADP; and c and f, 200 μM AMP. Square symbols, 10 mM $MgCl_2$, 20 mM KCl; circular symbols, 0.1 mM $MgCl_2$, 5 mM KCl; open symbols, minus adenine nucleotide; and filled symbols, plus adenine nucleotide.

mM Mg^{2+} and 25 mM K^+, conditions resembling the high-salt state. The specific rate at which the inactive, RuBP-bound Rubisco was activated was the same at activase concentrations of 1 and 4 μM (Fig. 9). Below 1 μM activase the specific rate of activation fell sharply. This rate was 50% at approximately 0.2 μM activase. Doubling the activity of the coupling enzymes in the assay had no significant effect on the rate of activation, confirming that the coupling system was not rate-limiting.

DISCUSSION

The specific activities of ADP release and intrinsic fluorescence enhancement exhibited similar dependencies on $MgCl_2$ and KCl concentrations (compare Fig. 2 with Fig. 5 and Fig. 3 with Fig. 6) in terms of the concentration range over which the response occurred. However, the profile of the response of ADP release was linear-hyperbolic, whereas that of intrinsic fluorescence enhancement was generally sigmoid. Thus, the 50% maximum response required higher Mg^{2+} and K^+ concentrations for ADP release than fluorescence (for $MgCl_2$, 1.3 and 0.8 mM, respectively; for KCl, 25 and 14 mM, respectively). The specific activities of ADP release and intrinsic fluorescence enhancement also responded in a similar fashion to the activase concentration (compare Figs. 4 and 7). Here the activase concentration required for 50% of the maximum response was higher for ADP release (about 0.24 μM) than for fluorescence enhancement (about 0.12 μM).

Mg^{2+} alone can promote intrinsic fluorescence enhancement with ATP-γ-S and the additional polymerization of activase that it represents, whereas K^+ requires a low concentration of added Mg^{2+} (Fig. 6). The maximum rates of ADP release and intrinsic fluorescence enhancement were both reached at about 5 mM $MgCl_2$ or 50 mM KCl. Thus, Mg^{2+} was more effective than K^+ by a factor of about 10. No attempt was made to free Rubisco activase entirely from Mg^{2+}. It may be presumed that the two tightly bound Mg^{2+} ions per activase monomer (Frasch et al., 1995) remained present on activase throughout the experiments reported here.

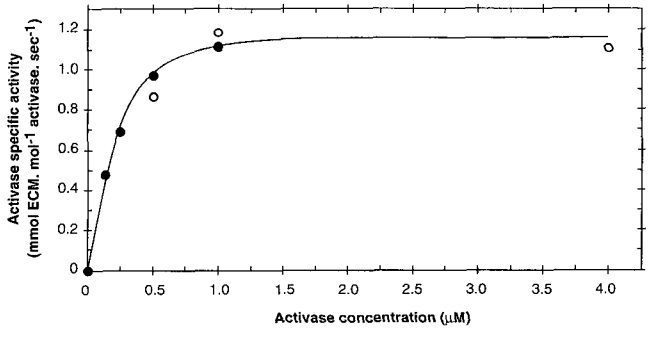

Figure 9. The effect of activase concentration on the rate of activation of RuBP-bound decarbamylated Rubisco. ○, Concentration of coupling enzymes as in "Materials and Methods"; ●, concentration of coupling enzymes doubled. The rates of spontaneous activation were determined and subtracted.

Since both ATPase and intrinsic fluorescence enhancement activities are related in some way to the extent of polymerization of Rubisco activase, it would be instructive to know the actual size of the dominant activase oligomer and the proportion of activase in the monomeric form for three conditions of particular interest that can be defined as follows: Condition a, high-salt and activase concentrations exceeding 1 μM; condition b, low-salt and activase concentrations exceeding 1 μM; and condition c, high-salt and activase concentrations below 0.1 μM.

Wang et al. (1993), using a Superose 6 column eluted in low-salt conditions with 20 mM bis-Tris-propane, 50 mM KCl, and 0.2 mM ATP (pH 8.0), found an apparent average molecular mass of 340 kD at 25°C. These conditions are comparable to those used in the experiment shown in Figure 6. With the addition of 5 mM Mg^{2+}, which gave conditions resembling those of high-salt, the apparent average molecular mass approximately doubled. However, the polymerization behavior at low activase concentrations (condition c) appears to favor dissociation to the monomer. Wang et al. (1993) found that the elution profile of activase eluted on Superose showed an asymmetric peak skewed toward the smaller size, consistent with the loss of monomeric activase from the trailing edge of the eluting activase band. Salvucci (1992) found an almost complete dissociation to the monomer in both long-term rate-zonal centrifugation and Sephacryl S-300 chromatography experiments with 10 mM $MgCl_2$. There is clearly insufficient evidence to assign polymerization states with confidence to the three conditions of interest defined here, and the proportion of monomeric activase present in each condition is unknown. However, it may be speculated from the foregoing that condition a is associated with a large oligomer of more than 14 subunits, condition b with a smaller oligomer of approximately 8 subunits, and condition c with a near-monomeric state.

The present results show that the extent of oligomerization of Rubisco activase, as determined by intrinsic fluorescence, is linked closely to the rate of release of ADP from ATP. This relationship holds when oligomerization from the inactive condition (b) to condition a is induced by increasing the concentration of Mg^{2+} at low K^+ (Figs. 2 and 5a), or by increasing the concentration of K^+ at low Mg^{2+} (Figs. 3 and 6). The effect of Mg^{2+} concentration on the rate of formation of Pi from ATP by Rubisco activase, reported by Frasch et al. (1995), is very similar to our data for ADP release (Fig. 2), extending this conclusion to the rate of release of Pi from ATP. When the activase concentration is decreased below 1 μM, fluorescence enhancement and ADP release are again similarly affected (Figs. 4 and 7) and the form predominant in condition c is also unable to hydrolyze ATP.

If the entire process of ATP hydrolysis is mediated by Rubisco activase in condition a (the large oligomer), it might be expected that activase will not bind the relevant adenine nucleotides under conditions in which this form is absent. However, the ANS fluorescence studies showed that Rubisco activase binds ATP-γ-S and ADP not only in the high-salt environment, but also in low-salt conditions

(b). AMP was not bound under either condition, demonstrating the specificity of this binding and supporting the validity of the technique. This immediately suggests a possible ATPase mechanism in which ATP is bound in exchange for ADP on the activase monomer, present in unknown proportions in all conditions. Hydrolysis of the bound ATP occurs only after polymerization of the ATP-bound monomer to form the large oligomer present in condition a, with the release of Pi but not ADP. The bound ADP is released only from the dissociated monomer in exchange for ATP (Fig. 10). Wang et al. (1993) noted that the aggregation of activase represents a "dynamic equilibrium" and it is likely that the dominant oligomeric form of activase is always accompanied by a small proportion of monomeric and other oligomeric forms.

The response of the ATPase activity of Rubisco activase to $MgCl_2$ and KCl and to dilution in high-salt conditions is strikingly similar to the behavior of actin. Actin, a single polypeptide of two major domains (Kabsch et al., 1990), has a molecular mass and amino acid residue numbers similar to Rubisco activase (e.g. in Arabidopsis both proteins are about 42 kD and have 377 residues). Like activase, the functional, tightly bound cation in actin is Mg^{2+} (Gershman et al., 1994), but the two proteins have low amino acid sequence homology (results not shown), precluding the utilization of sequence-structure comparison methods. With actin, the tightly bound metal ion and the bound adenine nucleotide are located in a cleft between the two major domains of the protein. The polymerization state of actin responds to $MgCl_2$ and KCl concentrations (Marumaya and Tsukagoshi, 1984) in a manner almost identical to Rubisco activase. Actin has an ATPase activity linked to the degree of polymerization (for reviews, see Stossel et al. [1985]; Pollard and Cooper [1986]; Pollard [1990]). Although actin is best known as a functional muscle protein, it is present in all eukaryote cells and has been identified in the chloroplast stroma (McCurdy and Williamson, 1987). Actin is recognized as a member of a functionally diverse group of proteins that share an ATPase domain of an identical three-dimensional structure, but low overall sequence homology (Bork et al., 1992). This group of proteins includes, in addition to actin, sugar kinases, hsp 70 heat-shock proteins, and prokaryotic cell cycle proteins.

The ATPase activity of actin is generally about 0.01 s^{-1} (Pollard, 1990). This is two orders of magnitude lower than Rubisco activase (although higher actin ATPase activities have been reported [Carlier et al., 1986]). This lower activity may reflect a relatively lower rate of initial nucleation of actin, resulting in its characteristic formation of relatively few but very long polymers. In comparison, the higher (1.0 s^{-1}) ATPase activity of Rubisco activase suggests more rapid nucleation, consistent with the observed formation of comparatively short oligomers of about 8- to 14-plus subunits (Salvucci, 1992; Wang et al., 1993). With actin, the relative rates of association of the ATP-bound monomer with the (+) ends of polymers, and of dissociation of the ADP-bound monomer from the (−) ends determine whether there is net polymer lengthening or shortening, but there is continual turnover or "treadmilling" of polymerized subunits at the expense of ATP. The ability of actin to polymerize is dependent on the actin concentration in the micromolar range (Marumaya and Tsukagoshi, 1984) and on the Mg^{2+} and K^+ concentrations, as we show here with Rubisco activase. This picture fits with all of the known properties of Rubisco activase if both polymerization of the ATP-bound monomer and release of the ADP-

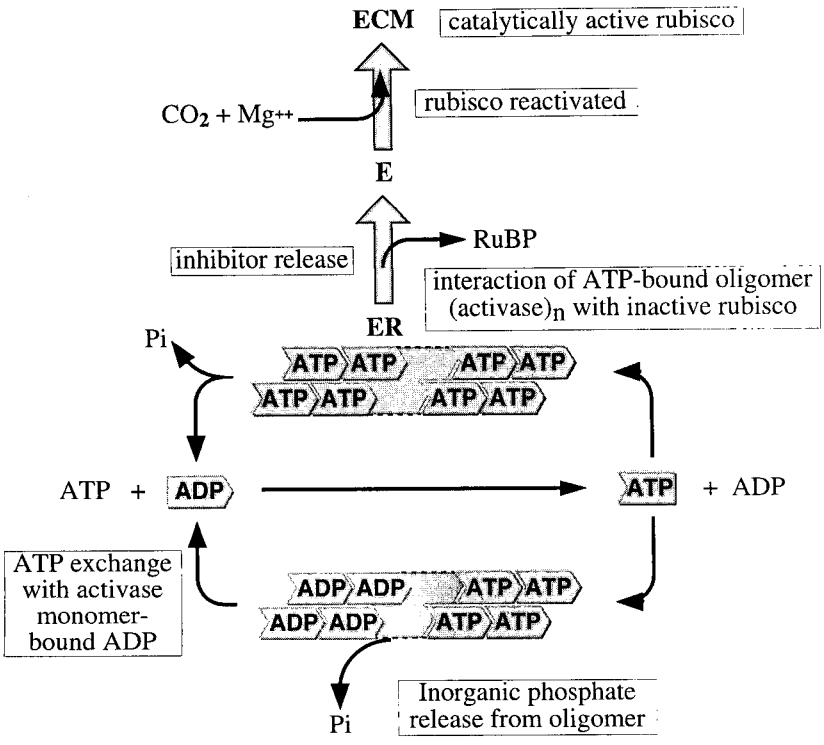

Figure 10. ATP-ADP exchange and ADP, Pi release by Rubisco activase by analogy with actin. Interaction of ATP-bound oligomeric activase species with inactivated Rubisco. ADP, ADP-bound monomer; ATP, ATP-bound monomer; ADP, ADP-bound subunit of oligomer; ATP, ATP-bound subunit of oligimer; ER, RuBP-bound decarbamylated Rubisco; E, decarbamylated Rubisco; ECM, carbamylated Rubisco.

bound monomer from activase oligomers (treadmilling) is fast compared with actin, resulting in the higher specific ATPase activity of Rubisco activase.

Wang et al. (1993) concluded that "increased aggregation of the protein induced by ATP and Mg^{2+} is an intermediate state between the binding of Mg-ATP and production of ADP." The present finding of similarity to actin supports and extends this conclusion, since binding of ATP to activase would be by exchange with ADP on the monomer. ATP hydrolysis with release of Pi but not ADP would occur on oligomer-bound subunits, and release of ADP by further exchange can occur only after dissociation of that monomer (Fig. 10).

The question then arises as to which form of activase interacts with hexose bisphosphate-bound decarbamylated Rubisco to release the bound inhibitor and allow Rubisco to bind activating CO_2 and Mg^{2+}. In the present study we show that the activase-specific activity for the Rubisco activation rate diminishes when the activase concentration is decreased to 125 nM (Fig. 9). These experiments were performed in the presence of 10 mM $MgCl_2$ and approximately 50 mM K^+, so that the decreasing activase concentration corresponds to a transition from condition a to condition c. Lan and Mott (1991) reported a linear relationship between the activase concentration and Rubisco activation rate, but they did not make measurements below about 500 nM activase. The decrease in the specific Rubisco activation rate shows that the form of activase that activates Rubisco is the large oligomer associated with condition a and speculated to be of 14-plus subunits. At 125 nM activase, the specific ATPase and intrinsic fluorescence enhancement are low as the protein approaches condition c, which we speculate corresponds to a near-monomeric form.

This finding implies that the type of interaction between activase and hexose bisphosphate-bound, decarbamylated Rubisco is with activase as an oligomer forming a framework that binds against and drives alterations in the conformation of parts of the large Rubisco holoenzyme, rather than a "crevice" in Rubisco into which an activase monomer or small oligomer would insert. Portis et al. (1995) have functionally identified one amino acid residue of several potential candidates on Rubisco that interacts with Rubisco activase. These residues map to the surface of the holoenzyme, forming an equatorial band (Portis, 1995), which, again, appears to favor a framework rather than a crevice mechanism for activase. These findings agree with the scheme of Andrews et al. (1995), in which activase undergoes a conformational change after binding to inactivated Rubisco, driving the retraction of the mobile loops that close over the hexose bisphosphate bound within the Rubisco active site, allowing its release. In this scheme, release of the products of normal catalysis starting with RuBP-bound carbamylated Rubisco results from conformational changes in Rubisco triggered by scission of the intermediate to the two monophosphate products.

Hammond et al. (1995) have determined an apparent rate constant for Rubisco activase of 0.993 nmol active sites.mg^{-1} activase.s^{-1}, using data obtained from tobacco leaves. This equates to a turnover of approximately 0.042 mol Rubisco active sites.mol^{-1} activase monomer.s^{-1}, which is slower by a factor of about 25 than the ATPase turnover rate determined here. For a hypothetical functional activase oligomer of 16 subunits, the turnover during Rubisco activation would be approximately 0.7 mol Rubisco active sites.mol^{-1} oligomer.s^{-1}.

Several authors have suggested mechanisms for the interaction of activase and the hexose bisphosphate-bound, decarbamylated Rubisco holoenzyme. Salvucci and Ogren (1996) discussed the molecular chaperone model for activase (Sanchez de Jimenez et al., 1995), pointing out the differences from GroE chaperonins, which, unlike activase, interact with unassembled and unfolded Rubisco subunits. Andrews et al. (1995) put forward a hypothetical model in which activase, after interaction with inactive Rubisco, which triggers the release of Rubisco-bound inhibitor, hydrolyzes ATP to regain its original conformation. Salvucci and Ogren (1996) suggested a slightly different scheme in which ATP binding promotes the interaction between activase and inactive Rubisco, with ATP hydrolysis occurring while the activase is bound to Rubisco.

If, however, as suggested here, Rubisco activase is an actin-like protein and a large oligomeric form is the species that interacts with inactive Rubisco, then the following model (Fig. 10) is suggestive. Activase monomers exchange bound ADP for ATP when the ATP/ADP quotient in the stroma is sufficiently high. The ATP-bound monomers assemble into a functional oligomer in the presence of suitable Mg^{2+} and K^+ concentrations. The stromal concentration of activase is far above 1 μM, so disassembly by dilution (as demonstrated here) is unlikely to occur in vivo. Illumination generates increases in the concentration of stromal Mg^{2+} (Gardemann et al., 1986) and the stromal ATP/ADP quotient (Stitt et al., 1982). This may only partially explain (Portis, 1992) the regulation of Rubisco activase by light. It should be noted that the stromal ATP/ADP quotient under illumination of about 3 (Stitt et al., 1982) is much lower than that achieved by in vitro ATP-regenerating systems such as those used here, and Rubisco activase in vivo may be limited to about 20% of its capacity by this factor (Robinson and Portis, 1989).

The oligomer of condition a interacts with the Rubisco holoenzyme, carrying one or more decarbamylated and inhibitor-bound sites, leading to hexose bisphosphate release. Hydrolysis of activase-bound ATP and release of Pi occur at points that cannot yet be precisely identified, but hydrolysis is likely to precede or accompany the activase-Rubisco-binding event because the nonhydrolyzable ATP analog, ATP-γ-S, promotes polymerization of Rubisco activase but inhibits Rubisco activation (Wang et al., 1993). Release of ADP-bound monomers from the oligomer occurs only after dissociation of activase from the reactivated Rubisco holoenzyme. If an oligomer assembled from the ATP-bound monomers fails to encounter a Rubisco holoenzyme carrying inactivated sites within a certain (unknown) time, spontaneous hydrolysis of the bound ATP, release of Pi, and, finally, of ADP-bound monomer occur, forming the

basis of the observed ATPase activity of Rubisco activase and corresponding to the well-known treadmilling of actin.

ACKNOWLEDGMENT

We thank Dr. Eric Larsen for providing spinach Rubisco and for useful discussions.

Received November 4, 1996; accepted February 27, 1997.
Copyright Clearance Center: 0032–0889/97/114/0605/09.

LITERATURE CITED

Andrews TJ, Hudson GS, Mate CJ, von Caemmerer S, Evans JR, Arvidsson YBC (1995) Rubisco: the consequences of altering its expression and activation in transgenic plants. J Exp Bot **46:** 1293–1300

Bork P, Sander C, Valencia A (1992) An ATPase domain common to prokaryotic cell cycle proteins, sugar kinases, actin, and hsp70 heat shock proteins. Proc Natl Acad Sci USA **89:** 7290–7294

Boyer PD (1962) Pyruvate kinase. *In* PD Boyer, H Lardy, K Myrback, eds, The Enzymes, Vol 6. Academic Press, New York, pp 95–113

Brooks A, Portis AR, Jr (1988) Protein-bound ribulose bisphosphate correlates with deactivation of ribulose bisphosphate carboxylase in leaves. Plant Physiol **87:** 244–249

Carlier M-F, Pantaloni D, Korn ED (1986) The effects of Mg^{2+} at the high-affinity and low-affinity sites on the polymerization of actin and associated ATP hydrolysis. J Biol Chem **261:** 10785–10792

Edmondson DL, Kane HJ, Andrews TJ (1990) Substrate isomerization inhibits ribulosebisphosphate carboxylase-oxygenase during catalysis. FEBS Lett **260:** 62–66

Frasch WD, Spano M, LoBrutto R (1995) VO^{2+} as a probe of metal binding sites in rubisco activase. *In* P Mathis, ed, Photosynthesis: from Light to Biosphere, Vol 5. Kluwer Academic Publishers, Dordrecht, The Netherlands, pp 257–260

Gardemann A, Schimkat D, Heldt HW (1986) Control of CO_2 fixation: regulation of stromal fructose-1, 6-bisphosphatase in spinach by pH and Mg^{2+} concentration. Planta **168:** 536–545

Gershman LG, Selden LA, Kinosian HJ, Estes JE (1994) Actin-bound nucleotide/divalent cation interactions. Adv Exp Med Biol **358:** 35–49

Hammond ET, Hudson GS, Andrews TJ, Woodrow IE (1995) Analysis of Rubisco activation using tobacco with antisense RNA to Rubisco activase. *In* P Mathis, ed, Photosynthesis: from Light to Biosphere, Vol V. Kluwer Academic Publishers, Dordrecht, The Netherlands, pp 293–296

Jordan DB, Chollet R (1983) Inhibition of ribulosebisphosphate carboxylase by substrate ribulose 1,5-bisphosphate. J Biol Chem **258:** 13752–13758

Kabsch W, Mannherz HG, Suck D, Pai EF, Holmes HC (1990) Atomic structure of the actin: DNase I complex. Nature **347:** 37–44

Lan Y, Mott KA (1991) Determination of apparent K_m values for ribulose 1,5-bisphosphate carboxylase oxygenase (Rubisco) activase using the spectrophotometric assay of Rubisco activity. Plant Physiol **95:** 604–609

Li L-A, Tabita FR (1994) Transcription control of ribulose bisphosphate carboxylase/oxygenase activase and adjacent genes in *Anabaena* species. J Bacteriol **176:** 6697–6706

Marumaya K, Tsukagoshi K (1984) Effects of KCl, $MgCl_2$, and $CaCl_2$ on the monomer-polymer equilibrium of actin in the presence and absence of Cytochalasin B. J Biochem **96:** 605–611

McCurdy DW, Williamson RE (1987) An actin-related protein inside pea chloroplasts. J Cell Sci **87:** 449–456

Pollard TD (1990) Actin. Curr Opin Cell Biol **2:** 33–40

Pollard TD, Cooper JA (1986) Actin and actin-binding proteins: a critical evaluation of mechanisms and functions. Annu Rev Biochem **55:** 987–1035

Portis AR, Jr (1990) Rubisco activase. Biochim Biophys Acta **1015:** 15–28

Portis AR, Jr (1992) Regulation of ribulose 1,5-bisphosphate carboxylase/oxygenase activity. Annu Rev Plant Physiol Plant Mol Biol **43:** 415–437

Portis AR, Jr (1995) The regulation of Rubisco by Rubisco activase. J Exp Bot **46:** 1285–1291

Portis AR, Jr, Esau B, Larson EM, Zhu G, Chastain CJ, O'Brien CM, Spreitzer RJ (1995) Characteristics of the interaction between rubisco and rubisco activase. *In* P Mathis, ed, Photosynthesis: from Light to Biosphere, Vol V. Kluwer Academic Publishers, Dordrecht, The Netherlands, pp 41–46

Robinson SP, Portis AR Jr (1989) Adenosine triphosphate hydrolysis by purified Rubisco activase. Arch Biochem Biophys **268:** 93–99

Robinson SP, Streusand VJ, Chatfield JM, Portis AR, Jr (1988) Purification and assay of Rubisco activase from leaves. Plant Physiol **88:** 1008–1014

Roesler KR, Ogren WL (1990) Primary structure of *Chlamydomonas reinhardtii* ribulose 1,5-bisphosphate carboxylase/oxygenase activase and evidence for a single polypeptide. Plant Physiol **94:** 1837–1841

Salvucci ME (1992) Subunit interactions of Rubisco activase: polyethylene glycol promotes self-association, stimulates ATPase and activation activities, and enhances interactions with Rubisco. Arch Biochem Biophys **298:** 688–696

Salvucci ME, Ogren WL (1996) The mechanism of Rubisco activase: insights from studies of the properties and structure of the enzyme. Photosynth Res **47:** 1–11

Salvucci ME, Werneke JM, Ogren WL, Portis AR, Jr (1987) Purification and species distribution of Rubisco activase. Plant Physiol **84:** 930–936

Sanchez de Jimenez E, Medrano L, Martinez-Barajas E (1995) Rubisco activase, a possible new member of the molecular chaperone family. Biochemistry **34:** 2826–2831

Shen JB, Orozco EM, Ogren WL (1991) Expression of the two isoforms of spinach ribulose 1,5-bisphosphate carboxylase activase and essentiality of the conserved lysine in the consensus nucleotide-binding domain. J Biol Chem **266:** 8963–8968

Stitt M, Lilley R McC, Heldt HW (1982). Adenine nucleotide levels in the chloroplasts, cytosol and mitochondria of wheat leaf protoplasts. Plant Physiol **70:** 971–977

Stossel TP, Chaponnier C, Ezzell RM, Harwig JH, Janmey PA, Kwiatkoski KJ, Lind SE, Smith DB, Southwick FS, Yin HL, Zaner KS (1985) Nonmuscle actin-binding proteins. Annu Rev Cell Biol **1:** 353–402

Wang Z-Y, Portis AR (1991) A fluorometric study with 1-anilinonaphthalene-8-sulfonic acid (ANS) of the interactions of ATP and ADP with Rubisco activase. Biochim Biophys Acta **1079:** 263–267

Wang Z-Y, Ramage RT, Portis AR (1993) Mg^{2+} and ATP or adenosine 5′-[γ-thio]-triphosphate (ATPγS) enhances intrinsic fluorescence and induces aggregation which increases the activity of spinach Rubisco activase. Biochim Biophys Acta **1202:** 47–55

Wang Z-Y, Snyder GW, Esau BD, Portis AR, Jr, Ogren WL (1992) Species-dependent variation in the interaction of substrate-bound Rubisco and Rubisco activase. Plant Physiol **100:** 1858–1862